

successive processes involved during calcination of oxyfluorinated templated compounds, such as defluorination, dehydration, and template decomposition, and predict the related calcined microporous structure. In these cases, we show that there is no need to describe the whole thermodynamic cycle to gain valuable information concerning the phase transformation of an as-synthesized compound into its related neutral framework in terms of energetics and structures. Such a method may not be applied to the specific cases where the calcination involves complex atomic rearrangements such as topotactic transformations, but in many cases, simulation is able to anticipate the solid-state transformation of an anionic molecular sieve into its related neutral framework. This is also the first time that our method gives accurate prediction of the solid-state transformation on a gallophosphate structure.

Received: November 2, 2001 [Z18147]

- [1] A. K. Cheetham, G. Férey, T. Loiseau, *Angew. Chem. Int. Ed.* **1999**, *38*, 3268; *Angew. Chem.* **1999**, *111*, 3466.
- [2] C. R. A. Catlow, *Computer Modelling in Inorganic Crystallography*, Academic Press, London, **1997**.
- [3] S. Girard, C. Mellot-Draznieks, J. D. Gale, G. Férey, *Chem. Commun.* **2000**, 1161.
- [4] T. Loiseau, C. Mellot-Draznieks, C. Sasse, S. Girard, N. Guillo, C. Huguenard, F. Taulelle, G. Férey, *J. Am. Chem. Soc.* **2001**, *123*, 9642.
- [5] ULM-6: N. Simon, T. Loiseau, G. Férey, *J. Chem. Soc. Dalton Trans.* **1999**, 7, 1147; CJ2: G. Férey, T. Loiseau, P. Lacorre, F. Taulelle, *J. Solid State Chem.* **1993**, *105*, 179.
- [6] S. Oliver, A. Kuperman, A. Lough, G. A. Ozin, *J. Mater. Chem.* **1997**, *7*, 807.
- [7] M. Estermann, L. B. McCusker, C. Baerlocher, A. Merrouche, H. Kessler, *Nature* **1991**, *352*, 320.
- [8] C. Sasse, T. Loiseau, F. Taulelle, G. Férey, *Chem. Commun.* **2000**, 943.
- [9] A. Simmen, J. Patarin, C. Baerlocher, *Proceedings of the 9th International Zeolite Conference*, Butterworth – Heinemann, Stoneham, **1993**, 433.
- [10] F. Taulelle, A. Samoson, T. Loiseau, G. Férey, *J. Phys. Chem. B* **1998**, *102*, 8588.
- [11] C. Schott-Daric, H. Kessler, M. Soular, V. Gramlich, E. Benazzi, *Stud. Surf. Sci. Catal.* **1994**, *84*, 101.
- [12] C. Baerlocher, W. M. Meier, D. H. Olson, *Atlas of Zeolite Framework Types*, Elsevier Science, Amsterdam, **2001**.
- [13] J. D. Gale, *J. Chem. Soc. Faraday Trans.* **1997**, *93*, 629.
- [14] J. D. Gale, N. J. Henson, *J. Chem. Soc. Faraday Trans.* **1994**, *90*, 3175.
- [15] S. Girard, J. D. Gale, C. Mellot-Draznieks, G. Férey, *Chem. Mater.* **2001**, *13*, 1732.
- [16] N. J. Henson, A. K. Cheetham, J. D. Gale, *Chem. Mater.* **1996**, *8*, 664.
- [17] G. Poulet, A. Tuel, P. Sautet, *Stud. Surf. Sci. Catal.* **2001**, *135*, 259.
- [18] A. Tuel, S. Caldarelli, A. Meden, L. B. McCusker, C. Baerlocher, A. Ristic, N. Rajic, G. Mali, V. Kaucic, *J. Phys. Chem. B* **2000**, *104*, 5697–5705.

## Assembly of a Face-to-Face Tetranuclear Copper(II) Complex as a Host for an Anthracene Guest\*\*

Raymond Ziessel,\* Loïc Charbonnière,  
Michèle Cesario, Thierry Prangé, and  
Hélène Nierengarten

The tailoring of sophisticated multitopic ligands that undergo metal-induced self-organization into well-defined architectures opens ways to the construction of organized supramolecular entities.<sup>[1]</sup> Such systems may display, at the molecular level, useful recognition and catalytic properties<sup>[2]</sup> and, at the macroscopic level, unusual mesomorphic<sup>[3]</sup> and electronic behavior.<sup>[4]</sup> Along these lines, it has been shown that rigid and linear polytopic ligands bearing bidentate chelating sites might self-assemble into well defined square-matrix arrays of metal centers without apparent defects following the general principle of maximum coordination.<sup>[5, 6]</sup> However, when flexible ligands are used the previous ideal situation is not effective anymore, instead, host–guest complexes have been characterized, in which an uncomplexed ligand is embedded into the structure.<sup>[7]</sup> The inclusion of a guest in a metal-containing architecture is an attractive property because it provides unique opportunities to study bimolecular reactions in microenvironments.<sup>[2, 8]</sup>

As a first step toward the catalytic transformation of guest molecules encapsulated in a macrocyclic groove containing photo- or electroactive metals, we report that the use of a ditopic phenanthroline (phen) ligand bearing a spiro[5.5]undecane spacer provides, upon complexation with copper(II) cations, a face-to-face arrangement together with an intertwined texture as minor species.

Here the self-inclusion of a free ligand is not observed but motion around the methylene linkage provides two types of supramolecular organization based on a linear or orthogonal arrangement of the phenanthroline subunits. Furthermore, the capability of the complex to exhibit an ideal cleft for flat polycyclic hydrocarbons prompted us to study the inclusion of

[\*] Dr. R. Ziessel, L. Charbonnière  
Laboratoire de Chimie Moléculaire, ECPM  
25 rue Becquerel, 67087 Strasbourg Cedex 02 (France)  
Fax: (+33) 3 90 24 26 89  
E-mail: ziessel@chimie.u-strasbg.fr

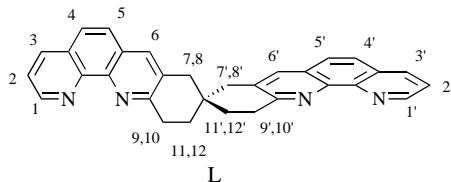
M. Cesario  
Institut de Chimie des Substances naturelles, CNRS  
91128 Gif-sur-Yvette (France)  
T. Prangé  
LURE Bât. 209d, Université Paris-Sud  
91405 Orsay (France)

H. Nierengarten  
Laboratoire de Spectrométrie de Masse Bio-organique, ECPM  
25 rue Becquerel, 67087 Strasbourg Cedex 02 (France)

[\*\*] This work was supported by the Centre National de la Recherche Scientifique and by the Engineering School of Chemistry (ECPM). Professor Randy Thummel is acknowledged for providing us a sample of ligand **L** (see ref. [9]) and Dr. Alain Van Dorsselaer for research facilities. We thank Dr. Mike Craig for reading the manuscript prior to publication and also Dr. Marc Ledoux for his expertise in the numeric processing of Figure 5.

anthracene, naphthalene, and pyrene within the macrocyclic structure.

The spiro-bridged bisphen ligand **L** (Scheme 1) was prepared by a Friedländer condensation between 8-amino-7-quinolinecarbaldehyde and 3,9-diketospiro[5.5]undecane as reported.<sup>[9]</sup> When ligand **L** was allowed to react with



Scheme 1. Numbering scheme of **L**.

one equivalent of  $[\text{Cu}(\text{CH}_3\text{CN})_4]\text{X}$  ( $\text{X} = \text{BF}_4, \text{ClO}_4, \text{PF}_6$ ) a deep-orange solution was instantaneously formed from which an orange–red solid precipitated upon the addition of diethyl ether. Elemental analysis data is consistent with  $\{\text{Cu}(\text{L})(\text{X})\}_n$  and the deep-orange color (UV/Vis:  $\lambda_{\text{max}} = 449 \text{ nm}$ ,  $\epsilon = 3220 \text{ mol}^{-1} \text{ dm}^3 \text{ cm}^{-1}$  per copper atom) arising from a metal-to-ligand charge transfer (MLCT) transition is characteristic of copper(I) surrounded in a tetrahedral fashion with four nitrogen atoms.<sup>[10]</sup>

Electrospray mass spectrometry (ES-MS) was a convenient analytical tool<sup>[11]</sup> to determine unambiguously the stoichiometry of this copper complex (Figure 1). Four peaks corresponding to the successive loss of  $\text{BF}_4^-$  ions are observed ( $m/z$  516.3 for  $[\text{Cu}_4\text{L}_4]^{4+}$ , 717.2 for  $[\text{Cu}_4\text{L}_4(\text{BF}_4)]^{3+}$ , 1119.2 for  $[\text{Cu}_4\text{L}_4(\text{BF}_4)_2]^{2+}$ , and 2325.0 for  $[\text{Cu}_4\text{L}_4(\text{BF}_4)_3]^+$ ). Furthermore, the isotopic pattern obtained for the most intense pseudo-molecular ion at  $m/z$  516.3 confirms the 4+ charge state of a tetranuclear complex. Interestingly, similar results are obtained using the  $\text{PF}_6^-$  and  $\text{ClO}_4^-$  salts.

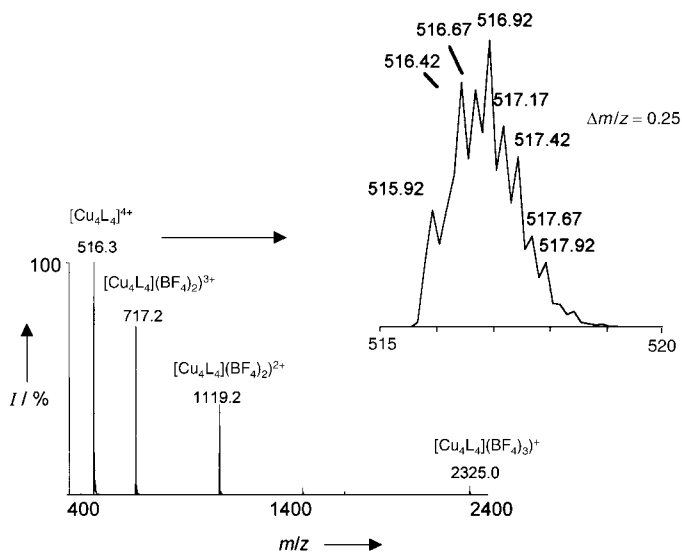


Figure 1. ES mass spectrum of an equimolar mixture of **L** and  $[\text{Cu}(\text{CH}_3\text{CN})_4]\text{BF}_4$  in  $\text{CH}_3\text{CN}$  ( $10^{-4} \text{ M}$ ) and isotopic pattern obtained for the peak at  $m/z$  516.3. Isotopic peaks are separated by 0.25  $m/z$  units confirming the charge state (4+) of the ion depicted in the insert.

From these data it becomes obvious that a cyclic tetranuclear complex of generic formula  $[\text{Cu}_4\text{L}_4](\text{BF}_4)_4$  was obtained. The different ways to intertwine the ligand around four tetrahedral metal centers are represented in Figure 2. While rigid bidentate ligands bearing parallel binding sites uniformly gave face-to-face structures of type **1**,<sup>[5,6]</sup> the introduction of flexibility between these sites or antiparallel binding vectors introduces new structures such as the plaited form **2**,<sup>[12]</sup> and the hybrid architectures **3** and **4**.<sup>[13]</sup>

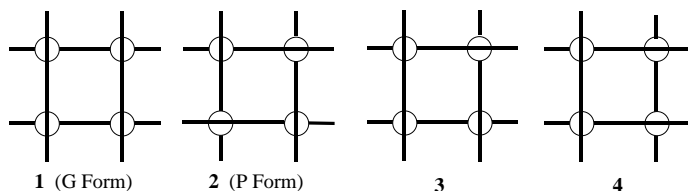


Figure 2. Possible ways of linking four tetrahedral metal centers (○) with four ligands **L**.

In  $\text{CD}_3\text{CN}$ , the  $^1\text{H}$  NMR spectrum of the isolated amorphous  $[\text{Cu}_4\text{L}_4](\text{BF}_4)_4$  material displays two families of protons (Figure 3b). The first family, which corresponds to the major

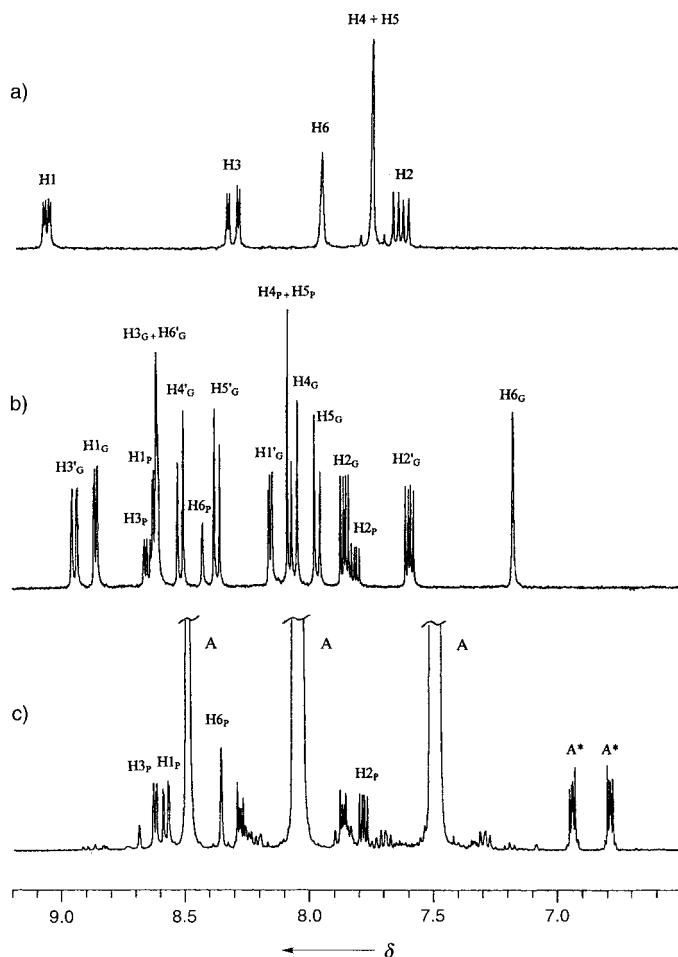


Figure 3.  $^1\text{H}$  NMR spectra of the aromatic part of a  $\text{CD}_3\text{CN}$  solution of: a) ligand **L**; b)  $[\text{Cu}_4\text{L}_4](\text{BF}_4)_4$ ; c)  $[\text{Cu}_4\text{L}_4](\text{BF}_4)_4$  in the presence of 30 equivalents of anthracene. Proton numbering corresponds to the numbering in Scheme 1 with G and P for the face-to-face and plaited structures, respectively, A = free anthracene, A\* = intercalated anthracene.

species, comprised 12 signals from aromatic and 12 from aliphatic protons all integrating for one proton, while the second set displayed 10 resonance signals with the same integral values and a peak of twice this value. Simple symmetry considerations rapidly eliminate possibilities **3** and **4** (Figure 2) as a result of the inherent lack of symmetry elements. The presence of a spirobicyclic spacer between the two phen subunits precludes the possibility of vertical planes of symmetry in structure **1** giving an overall  $D_2$  symmetry group which leads to 12 resonance signals for the aromatic protons. With all six methylene groups being stereotopic, 12 resonance signals from aliphatic hydrogen atoms are expected and are indeed observed. For the minor species, a plaited structure **2** is suggested, because of the presence of a set of two  $C_2$  axes perpendicular to the main axis and passing through the spiro carbon atoms, thus leading to a  $D_4$  symmetry group. Consequently, the number of nonequivalent aromatic protons is reduced to six. Full assignment of the protons of the ligand in each family was achieved by two-dimensional (2D) COSY and NOESY experiments (Table 1).

Table 1. Chemical shift values for the protons of the ligand in the face-to-face structure **1**, the plaited structure **2** and the free ligand L.<sup>[a]</sup>

Proton	Form 1	Form 2	Free ligand L
H1	8.87	8.16 <sup>[b]</sup>	8.64
H2	7.86	7.60 <sup>[b]</sup>	7.68
H3	8.62	8.95 <sup>[b]</sup>	8.35
H4	8.06	8.52 <sup>[b]</sup>	7.80
H5	7.97	8.38 <sup>[b]</sup>	7.80
H6	7.18	8.61 <sup>[b]</sup>	8.00
H7, H8	0.62, 2.67	2.17, 2.75 <sup>[b]</sup>	3.08, 3.23
H9, H10	1.70, 1.24	−0.31, 2.70 <sup>[b]</sup>	2.97, 1.53
H11, H12	1.35, 2.21	0.74, 2.37 <sup>[b]</sup>	1.71, 2.20

[a] The numbering scheme is provided in Scheme 1. [b] Refers to the part of the molecules numbered with a prime.

In the face-to-face structure **1**, the two phen subunits of a single ligand can be distinguished. Some drastic upfield shifts can be observed with respect to the free ligand (see H6<sub>G</sub>, H7<sub>G</sub>, H9<sub>G</sub>, and H11<sub>G</sub> in Table 1 and Figure 3); it is surmised that those protons are located in the shielding region of a neighboring spiro-phen molecule. Nuclear Overhauser enhancement (NOE) correlations between H6<sub>G</sub> and H4'<sub>G</sub>, H6<sub>G</sub> and H3'<sub>G</sub>, and H5<sub>G</sub> and H3'<sub>G</sub> revealed dipolar interactions between the phen subunits corresponding to interactions with two ligands in a parallel configuration of type **1**. Assuming that the thermodynamic equilibrium was reached during the assembly process leading to the tetranuclear complexes, the ratio of both structures allows for calculation of the energy difference and shows the face-to-face structure to be 3.8 kJ mol<sup>−1</sup> more stable than the plaited structure. Furthermore, field-dependent measurements and saturation-transfer experiments did not reveal any chemical exchange between these structures and a lower limit of 73.3 kJ mol<sup>−1</sup> can be calculated for the activation energy necessary for chemical exchange between the two forms.

The crystal structure of the major complex unambiguously confirms a tetranuclear macrocyclic arrangement and the asymmetric unit consists of discrete [Cu<sub>4</sub>L<sub>4</sub>]<sup>4+</sup> and PF<sub>6</sub><sup>−</sup> ions (Figure 4a).<sup>[14]</sup> The overall scaffold is a face-to-face structure

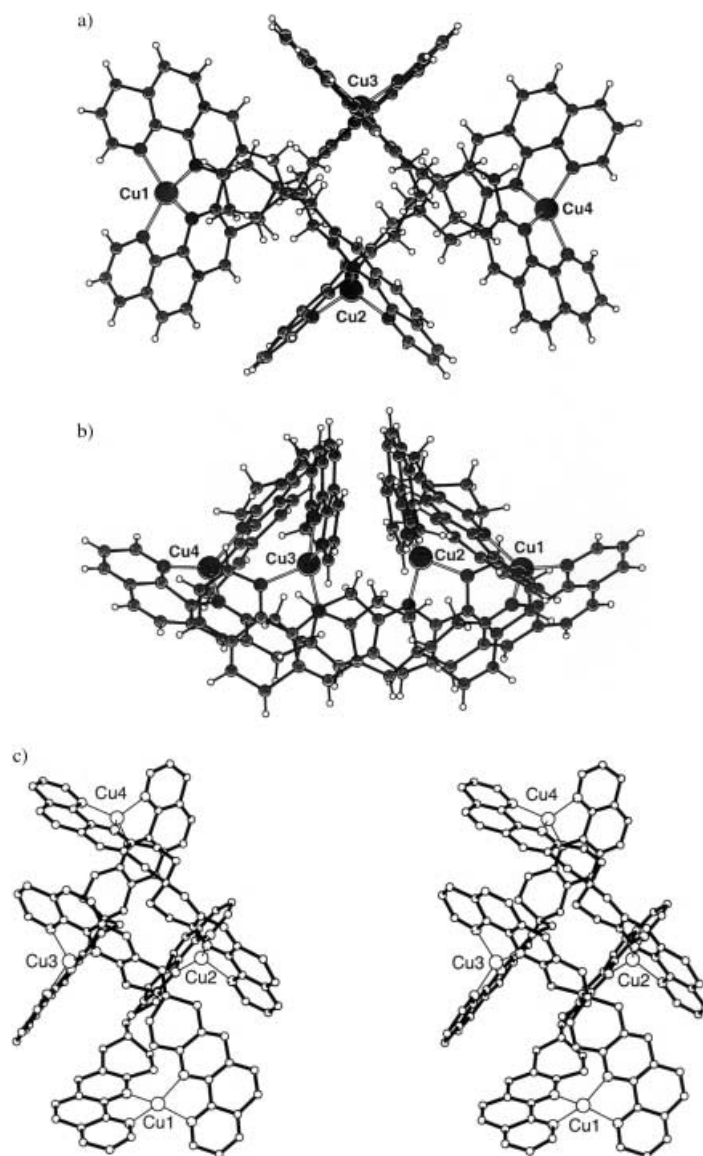


Figure 4. ORTEP representations of the tetranuclear [Cu<sub>4</sub>L<sub>4</sub>]<sup>4+</sup> complex: a) view along the pseudo- $C_2$  axis of the molecule; b) view orthogonal to the  $C_2$  axis of the molecule; c) stereoview.

where the four copper atoms are tetrahedrally coordinated to two phen subunits belonging to two independent ligands. The four metal centers provide a quasi-planar arrangement with a root-mean-square deviation of 0.151(2) Å. Within this plane, the copper(II) ions are placed at the vertices of a rhombus of edge 8.5 Å, with an acute angle of 52°. Two kinds of distinct coordination for the copper atoms are found. For Cu1 and Cu4, placed at acute angles of the rhombus, the dihedral angles formed by the two coordinated phen mean planes (74.3 and 78.6°, respectively) reflect a flattening of the coordination tetrahedron, while for Cu2 and Cu3, the angles (91.5 and 88.6°, respectively) are very close to a conventional right angle. In a single ligand strand, the average dihedral angles defined by the phen mean planes vary around 49° (from 44–53°). The tetranuclear complex adopts a basket-shaped conformation (Figure 4b). The largest dimensions of the basket are 21.6 Å between the most extreme phen units and

9.0 Å in height. A striking result revealed by the crystal structure is the presence of a large pocket of about  $7.4 \times 8.8 \text{ Å}^2$ , auspicious for the intercalation of planar substrates. A stereoview of the molecular structure is provided in Figure 4c.

A very interesting feature was observed by  $^1\text{H}$  NMR spectroscopy, upon addition of excess anthracene the signals corresponding to the face-to-face structure drastically decrease and a plethora of new signals are seen, while signals corresponding to the plaited structure remain unchanged (Figure 3c). Furthermore, a new set of three signals can be observed at  $\delta = 6.93$ , 6.78 (Figure 3c), and 4.57 (not shown) integrating for two, two, and one protons, respectively. NOE differential experiments show these signals to be chemically exchangeable with those of anthracene, which suggests that they correspond to anthracene molecules in a particular chemical environment. Furthermore, assuming these new signals are from anthracene molecules, their integral values correspond, within experimental error, to the loss in intensity observed for the signals of the face-to-face structure. These results suggest that this latter structure can act as a host for one anthracene molecule (Figure 5b). This process, probably driven by  $\pi$ -stacking interactions with some phenanthroline subunits, causes large upfield shifts of the signals belonging to the intercalated guest and also leads to the disruption of the overall symmetry of the superstructure. This loss of symmetry results in a splitting of the original signals of the face-to-face compound into numerous new peaks ( $\delta = 7.17\text{--}7.38$ ,  $7.66\text{--}7.73$ ,  $7.82\text{--}7.91$ ,  $8.17\text{--}8.30$ , Figure 3c) some of them being hidden by the intense anthracene signals. In contrast, the plaited structure does not allow inclusion of anthracene and its signals remain unperturbed. An estimated value of  $(5.8 \pm 0.9) \text{ M}^{-1}$  was calculated for the association of anthracene within the face-to-face structure.

To confirm the presence of electronic interaction between the macrocyclic host and the anthracene guest, cyclic voltammetric (CV) studies of solutions of the  $\text{PF}_6$  complex were carried out. The tetranuclear complexes undergo a single but broad oxidative process at +0.56 V (full details of the CV experiment are in the Experimental Section) consistent with the oxidation of copper(I) to copper(II). The relatively high oxidative potential found for this complex is in keeping with those found for various copper(I)–phen compounds.<sup>[15]</sup> The relatively large  $\Delta E_p$  ( $\Delta E_p = E_p^a - E_p^c$ ) for the oxidation wave (ca. 100 mV) indicates that it may result from multiple closely

spaced one-electron oxidations of each metal center. In addition, two ligand-based reductions at  $-1.48 \text{ V}$  ( $\Delta E_p = 65 \text{ mV}$ ) and  $-1.72 \text{ V}$  ( $\Delta E_p = 72 \text{ mV}$ ) are ascribed to the sequential reductions of each phen subunit surrounding the copper(I) centers. Each of these reduction peaks corresponds to four electrons compared to the four electrons released during the oxidation process. By adding 10–30 equivalents of anthracene no significant shifts of the copper-based oxidation and the first ligand-localized reduction could be observed, but the second ligand-based reduction shifted by 100 mV with a marked broadening of the redox wave. This observation is in keeping with the intercalation of anthracene which results in the increase of the electron density of the interacting phen fragments and consequently in a large cathodic shift. Attempts to determine the reduction potential of the encapsulated anthracene (above  $-1.95 \text{ V}$ ) were hampered by the use of a large excess of anthracene.

In conclusion, the results presented here provide a rational approach for the engineering of molecular scaffoldings. The introduction of moderate flexibility into the linkage between two phen subunits produced the inorganic face-to-face arrangement as the major species while tilting of the binding vectors provide a plaited arrangement (Figure 5a and 5c, respectively) Because of the size of the spiro ligand and the steric constraints imposed by the [5·5] linkage the  $\pi$  stacking of the phen units is not optimal, which leaves, in the face-to-face arrangement, open space for interaction with added cyclic aromatic guests, such as anthracene, naphthalene, or pyrene. The molecular recognition event has been investigated by cyclic voltammetry as well as by proton NMR spectroscopy which also show that in the plaited species the recognition of anthracene is not effective. This result is used to confirm the parallel configuration of the ligands in the major compound, a configuration confirmed by the solid-state X-ray structure. Copper(I)–phen complexes exhibit oxidative nucleic acid activity<sup>[16]</sup> and because of the presence of similar centers in the present species, the capability to act as a microreactor for the catalytic oxygenation of the encapsulated anthracene guest is currently under investigation.

#### Experimental Section

ES-MS measurements were performed on a triple quadrupole mass spectrometer Quattro II (Micromass, Altrincham, UK). The ES source was heated to  $80^\circ\text{C}$ . The sampling cone voltage ( $V_c$ ) was at 20 V to avoid any fragmentation processes. Sample solutions were introduced into the



Figure 5. Photographs of the Corey–Pauling–Koltun (CPK) molecular models of the tetranuclear complexes representing a) the face-to-face arrangement in perfect keeping with the X-ray structure; b) encapsulation of an anthracene substrate in the previous face-to-face arrangement; c) the plaited organization obtained by motion around the  $\text{CH}_2$  linkage of the spiro linkers.

mass spectrometer source with a syringe pump (Harvard type 551111: Harvard Apparatus Inc., South Natick, MA, USA) with a flow rate of  $4 \mu\text{L min}^{-1}$ . Calibration was performed using protonated horse myoglobin. Scanning was performed in the MCA (multichannel analyzer) mode, and several scans were combined to obtain the final spectrum. Electrochemical studies were made by cyclic voltammetry with a conventional three-electrode system using a BAS CV-50 W voltammetric analyzer equipped with a Pt microdisk or a Hg Kemula hanging electrode as working electrode and a Ag wire counter electrode. Ferrocene ( $E_{1/2} = +0.65 \text{ V}$ ) or paraquat ( $E_{1/2} = -0.23$  and  $-0.60 \text{ V}$ ) were used as an internal standard with the Pt and Hg electrodes, respectively. Solutions contained the electrode-active substrate (ca.  $5 \times 10^{-4} \text{ mol dm}^{-3}$ ) in deoxygenated and anhydrous DMF containing tetra-*N*-butylammonium tetrafluoroborate ( $0.2 \text{ mol dm}^{-3}$ ) as supporting electrolyte. The quoted half-wave potentials were reproducible within  $15 \text{ mV}$ .

Received: November 2, 2001 [Z18146]

- [1] R. W. Saalfrank, I. Bernt, *Curr. Opin. Solid State Mater. Sci.* **1998**, *3*, 407–413; M. Munakata, L. P. Wu, T. Kuroda-Sowa, *Adv. Inorg. Chem.* **1999**, *46*, 173–303; M. Fujita, *Acc. Chem. Res.* **1999**, *32*, 53–61; D. L. Caulder, K. N. Raymond, *Acc. Chem. Res.* **1999**, *32*, 975–982; C. Piguet, *J. Inclusion Phenom. Macrocyclic Chem.* **1999**, *34*, 361–391; M. Albrecht, *J. Inclusion Phenom. Macrocyclic Chem.* **2000**, *36*, 127–151; A. von Zelewsky, O. Mamula, *J. Chem. Soc. Dalton Trans.* **2000**, 219–231.
- [2] J. Kang, J. Rebeck, Jr., *Nature* **1997**, *385*, 50–52.
- [3] A. El-ghayoury, L. Douce, A. Skoulios, R. Ziessel, *Angew. Chem.* **1998**, *110*, 2327–2331; *Angew. Chem. Int. Ed.* **1998**, *37*, 2205–2208.
- [4] C. P. Collier, E. W. Wong, M. Belohradsky, F. M. Raymo, J. F. Stoddart, P. J. Kuekes, R. S. Williams, J. R. Heath, *Science* **1999**, *285*, 391–394; C. P. Collier, G. Mattersteig, E. W. Wong, Y. Luo, K. Kristen, J. Sampaio, F. M. Raymo, J. F. Stoddart, J. R. Heath, *Science* **2000**, *289*, 1172–1175.
- [5] M.-T. Youinou, N. Rahmouni, J. Fischer, J. A. Osborn, *Angew. Chem.* **1992**, *104*, 771–773; *Angew. Chem. Int. Ed. Engl.* **1992**, *31*, 733–735; P. Baxter, J.-M. Lehn, J. Fischer, M.-T. Youinou, *Angew. Chem.* **1994**, *106*, 2432–2435; *Angew. Chem. Int. Ed. Engl.* **1994**, *33*, 2284–2287.
- [6] M. Ruben, E. Breuning, J.-P. Gisselbrecht, J.-M. Lehn, *Angew. Chem.* **2000**, *112*, 4312–4315; *Angew. Chem. Int. Ed.* **2000**, *39*, 4139–4142; A. M. Garcia, F. J. Romero-Salguero, D. M. Bassani, J.-M. Lehn, G. Baum, D. Fenske, *Chem. Eur. J.* **1999**, *5*, 1803–1808; J. R. Galan-Mascaros, K. R. Dunbar, *Chem. Commun.* **2001**, 217–218; C. S. Campos-Fernandez, R. Clérac, K. R. Dunbar, *Angew. Chem.* **1999**, *111*, 3685–3688; *Angew. Chem. Int. Ed.* **1999**, *38*, 3477–3479.
- [7] S. Toyota, C. R. Woods, M. Benaglia, R. Haldimann, K. Wärnmark, K. Hardcastle, J. S. Siegel, *Angew. Chem.* **2001**, *113*, 773–776; *Angew. Chem. Int. Ed.* **2001**, *40*, 751–754.
- [8] M. Yoshizawa, T. Kusukawa, M. Fujita, K. Yamaguchi, *J. Am. Chem. Soc.* **2000**, *122*, 6311–6312.
- [9] F. Wu, E. C. Riesgo, R. P. Thummel, A. Juris, M. Hissler, A. El-ghayoury, R. Ziessel, *Tetrahedron Lett.* **1999**, *40*, 7311–7314; A. Juris, L. Prodi, A. Harriman, R. Ziessel, M. Hissler, A. El-ghayoury, F. Wu, E. C. Riesgo, R. P. Thummel, *Inorg. Chem.* **2000**, *39*, 3590–3598.
- [10] R. M. Everly, R. Ziessel, J. Suffert, D. R. McMillin, *Inorg. Chem.* **1991**, *30*, 559–561; A. Juris, R. Ziessel, *Inorg. Chim. Acta* **1994**, *225*, 251–254, and references therein.
- [11] A. Rigault-Marquis, A. Dupont-Gervais, P. N. W. Baxter, A. Van-Dorsselaer, J.-M. Lehn, *Inorg. Chem.* **1996**, *35*, 2307–2310.
- [12] T. Bark, M. Dügge, H. Stoeckli-Evans, A. von Zelewsky, *Angew. Chem.* **2001**, *113*, 2924–2927; *Angew. Chem. Int. Ed.* **2001**, *40*, 2848–2851.
- [13] R. Ziessel, *Coord. Chem. Rev.* **2001**, *216/217*, 195–223.
- [14] Crystal data for  $[\text{Cu}_4\text{L}_4](\text{PF}_6)_4$ :  $\text{C}_{124}\text{H}_{96}\text{Cu}_4\text{N}_{16}\text{P}_4\text{F}_{24}$ ,  $M_r = 2644.21$ ; deep-orange diamond-shaped microplates ( $0.2 \times 0.2 \times 0.02 \text{ mm}^3$ ), obtained by slow evaporation of an acetonitrile solution.  $\mu = 0.778 \text{ mm}^{-1}$ ,  $F(000) = 5376$ , monoclinic, space group  $C2$ ,  $a = 26.645(4)$ ,  $b = 16.607(3)$ ,  $c = 29.359(4) \text{ \AA}$ ,  $\beta = 91.7(1)^\circ$ ,  $V = 13065.1 \text{ \AA}^3$ ,  $Z = 4$ ,  $\rho_{\text{calc}} = 1344 \text{ kg m}^{-3}$ . Data collection at  $277(2) \text{ K}$  on the wiggler line DW32 (R. Fourme, P. Dhez, J. P. Benoit, R. Kahn, P. Dubuisson, J.

Frouin, *Rev. Sci. Instrum.* **1992**, *63*, 982–987) at the DCI synchrotron, LURE (Orsay-France) at  $\lambda = 0.964 \text{ \AA}$ , on a MAR-Research 345 image plate system. Image plate distance:  $10 \text{ cm}$ . A total of 100 frames, each  $3^\circ$  in rotation, were recorded and processed with the *hkl* package of the program (Z. Otwinowski, W. Minor, *Methods Enzymol.* **1997**, *276*, 307–326). As one of the twins was in greater percentage, it was possible to integrate only one component at the indexing level.  $3.74 < \theta < 26.26^\circ$ ,  $-24 \leq h \leq 24$ ,  $0 \leq k \leq 15$ ,  $0 \leq l \leq 27$ . A total of 23225 reflections was obtained of which 5490 were independent and used to refine 809 parameters. 5462 observed reflections with  $I > 2\sigma(I)$ .  $R = 0.0961$ ,  $wR_2 = 0.2578$  (observed),  $R = 0.0964$ ,  $wR_2 = 0.2580$  (all data). The structure was solved by direct methods (SHELXS86) and refined on  $F^2$  for all reflections by least-squares method (SHELXS93). Hydrogen atoms were introduced at their theoretical positions and refined with constraints on bond distances and angles. Isotropic thermal factors were kept at 1.2 times that of the bonded atom. Only copper, nitrogen, and phosphorus atoms were refined anisotropically to limit the number of parameters versus the number of data. Largest difference peak and hole are  $0.82$  and  $-0.57 \text{ e \AA}^{-3}$ , respectively. CCDC-170600 contains the supplementary crystallographic data for this paper. These data can be obtained free of charge via [www.ccdc.cam.ac.uk/conts/retrieving.html](http://www.ccdc.cam.ac.uk/conts/retrieving.html) (or from the Cambridge Crystallographic Data Centre, 12, Union Road, Cambridge CB2 1EZ, UK; fax: (+44) 1223-336-033; or [deposit@ccdc.cam.ac.uk](mailto:deposit@ccdc.cam.ac.uk)).

- [15] C. Dietrich-Buchecker, J.-P. Sauvage, J.-M. Kern, *J. Am. Chem. Soc.* **1989**, *111*, 7791–7800.
- [16] D. S. Sigman, *Acc. Chem. Res.* **1986**, *19*, 180–186, and references therein.

## The Mechanism of Catalytic Enantioselective Fluorination: Computational and Experimental Studies

Stefano Piana, Ingrid Devillers, Antonio Togni,\* and Ursula Rothlisberger\*

Despite the undisputed importance of organofluorine compounds, for example, in biomedical applications, the generation of fluorinated carbon stereocenters by C–F bond-forming reactions remains rare and particularly challenging.<sup>[1,2]</sup> Recently, the first catalytic, enantioselective fluorination of  $\beta$ -ketoesters with F-TEDA (1-chloromethyl-4-fluoro-1,4-diazoniabicyclo[2.2.2]octane; TEDA = triethylenediamine) in the presence of 5% of  $[\text{TiCl}_2(\text{TADDOLato})]$  (TADDOL =  $\alpha, \alpha', \alpha'$ -tetraaryl-2,2-dimethyl-1,3-dioxolan-4,5-dimethanol) catalysts was reported.<sup>[3,4]</sup> We have shown that the reaction proceeds smoothly in acetonitrile at room temperature and the obtained enantioselectivity reaches 90% *ee* using a (*R,R*)-TADDOL bearing 1-naphthyl substituents.<sup>[4]</sup> We assume, as a first mechanistic hypothesis, that

[\*] Prof. Dr. A. Togni, Prof. Dr. U. Rothlisberger, Dr. S. Piana, Dr. I. Devillers  
Laboratory of Inorganic Chemistry  
Swiss Federal Institute of Technology, ETH Hönggerberg  
8093 Zürich (Switzerland)  
Fax: (+41) 1-632-1090  
E-mail: [togni@inorg.chem.ethz.ch](mailto:togni@inorg.chem.ethz.ch), [uro@inorg.chem.ethz.ch](mailto:uro@inorg.chem.ethz.ch)

Supporting information for this article is available on the WWW under <http://www.angewandte.com> or from the author.